Analytical Study on Soot Formation in a Diesel Engine

Sangsu Lee
Technical Center, GM Daewoo Auto&Technology Co., Incheon, Korea
Nakwon Sung*, Jeongmin Lee
School of Mechanical Engineering, Sungkyunkwan University, Suwon, Korea
Hongsuk Kim
Engine Research Center, Korea Institute of Machinery and Materials, Daejeon, Korea

The soot formation inside a diesel engine was studied by the analytical model. The soot is formed from gaseous carbon atoms by the phase change under the saturation condition. This soot model is implemented into the KIVA-3V code. From the results of the model, it is found that the fuel rich core of spray inside a flame is the main source of soot. The effect of injection timing is investigated by the soot model. When the injection timing is advanced, the formation of soot is suppressed because of high saturation pressure. The soot formation is increased when the injection timing is retarded mainly due to the decreased soot oxidation at low cylinder temperature.

Key Words : Diesel Engine, KIVA-3V, Soot model, Soot Inception, Soot Oxidation, Phase Equilibrium, Injection Timing, Precursor

1. Introduction

Although diesel engines have higher thermal efficiency than gasoline engines, they emit more exhaust gases containing NOx and soot. Many researchers are aimed to reduce the diesel emissions by improving combustion in the engine and using the aftertreatment devices. For the research of engine, it is necessary to develop a 3D model of diesel cycle which has fuel injection, combustion and emission formations inside a cylinder. The NO formation inside a diesel engine has been well described by Zeldovich (Heywood, 1988). However, the soot formation inside a diesel engine was not fully understood yet. Hiroyasu and Nishida (1989) proposed a simple model for soot formation which calculates pyrolysis of fuel into the soot particles. The results from the model are well matched with the experimental data over the wide engine operating conditions. Surovikin (1976) used molecular collision theory for the soot formation. In his method, the radicals are produced by pyrolysis of fuel. Then, soot is formed from the radicals and grows with addition of fuel molecules into the surface of soot. Hampson (1997) applied Surovikin's model to the diesel engine, and found that the model was not as predictive as the Hiroyasu model. Kazakov and Foster (1998) explained formation of soot by the multi step mechanisms. His model includes the processes of inception, coagulation, growth and oxidation of soot particles. Frenklach (2002) explained soot formation by polycyclic aromatic hydrocarbons (PAH). In his model, soot particles are generated by collisions between PAH and grown by the abstraction of

* Corresponding Author,
E-mail : nwsung@skku.edu
TEL : +82-10-3015-7439; **FAX** : +82-31-295-1937
School of Mechanical Engineering, Sungkyunkwan University, Suwon, Korea. (Manuscript **Received** April 3, 2006; **Revised** October 26, 2006)

hydrogen atom and the addition of acetylene on soot surface. This model is quite informative on soot formation, but requires much computational efforts for hundreds of species under consideration.

In this study, the soot inception is calculated from the phase change of gaseous carbon atoms to solid soot particles under the saturation condition. The initial soots are then grown by the acetylene and undergo coagulations during collisions. Most of the soots are oxidized and survived soots are emitted from the engine. The purpose of this study is to understand the mechanism of soot formation in the engine. By the developed model, the effects of injection timing on the soot formation are investigated.

2. Soot Formation Model

The formation of soot can be explained by a series of processes such as soot inception, surface growth, particle coagulation and particle oxidation. There are many descriptions for each process by chemical reactions (Kazakov and Foster, 1998; Leung and Lindstedt, 1991; Liu et al., 2002; Tao et al., 2004). In this study, the soot model proposed by Foster et al. was used which had 9 chemical reactions for soot formation (Kazakov and Foster, 1998). The soot is initiated from gaseous carbon atoms produced during combustion. The carbon radicals form a precursor for soot. For calculation, the precursor is assumed to be C_{50}.

$$C_{14}H_{30} \Rightarrow 0.28PR + 15H_2 \tag{1}$$

and its rate is

$$r_1 = A_1 \exp(-T_1/T)\, Y_F \tag{2}$$

Table 1 lists constants used for the chemical reactions. The acetylene is also generated from fuel by pyrolysis,

$$C_{14}H_{34} \Rightarrow 7C_2H_2 + 8H_2 \tag{3}$$

The reaction rate is given by

$$r_2 = A_2 \exp(-T_2/T)\, Y_F \tag{4}$$

In the Foster model, the precursors are converted to the soot particle by the chemical reaction (Kazakov and Foster, 1998),

Table 1 Arrhenius parameters used in soot model

No.	A_i (mol,cm,K,s)	T_i (K)	Ref.
1	9.25e+10	60419	Kazakov and Foster, 1998
2	3.93e+8	24671	Kazakov and Foster, 1998
3	1.0e+10	25174	Kazakov and Foster, 1998
4	6.0e+3	12100	Leung and Lindstedt, 1991
6	1.0e+12	20140	Kazakov and Foster, 1998
7	6.0e+13	25178	Kazakov and Foster, 1998

$$PR \Rightarrow soot \tag{5}$$

$$r_3 = A_3 \exp(-T_3/T)\, Y_{PR} \tag{6}$$

Contrary to the chemical reaction theory, the concept of phase equilibrium is used for the inception of soot. The precursors are converted to the soot particles when the partial pressure of the precursors in the gaseous mixture exceeds saturation pressure at the given temperature. The pressure-temperature diagram of carbon in Fig. 1 is used for calculating the saturation pressure of the precursors at the given temperature (Pierson, 1993). When the precursors are produced during combustion, the partial pressure of the precursors in the products is increased and reaches the saturation pressure. Then, the precursors begin to be transformed into the solid soot particles. The mass fraction of gaseous precursors in the products at saturation state is

$$Y_{SAT} = \frac{P_{SAT}}{P}\frac{W_{PR}}{W_{mix}} \tag{7}$$

The rates of change of the precursors, soot and soot number density due to formation are determined,

$$\left.\frac{dY_{PR}}{dt}\right|_{INC} = -\frac{Y_{PR} - Y_{SAT}}{\Delta t} \tag{8}$$

$$\left.\frac{dY_{soot}}{dt}\right|_{INC} = \frac{Y_{PR} - Y_{SAT}}{\Delta t} \tag{9}$$

$$\left.\frac{dN}{dt}\right|_{INC} = \frac{\rho N_A}{W_{PR}}\left.\frac{dY_{soot}}{dt}\right|_{INC} \tag{10}$$

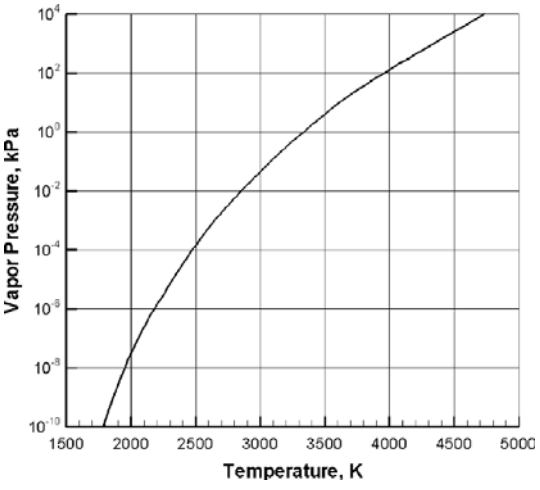

Fig. 1 Vapor pressure of carbon (Pierson, 1993)

where W_{PR} is the molecular weight of the precursor, 600 g/mole.

The more precursors are transformed into the soot particles when the cylinder temperature is decreased or the partial pressure of the precursor is increased. The initial soot particle is assumed to have 50 carbon atoms with the size of 1 nm in diameter.

Acetylene adds carbon atoms to the surface of soot,

$$Soot + C_2H_2 \Rightarrow \text{“}Bigger\ soot\text{”} + H_2 \tag{11}$$

$$r_4 = A_4 \exp(-T_4/T)\, S^{1/2}\, Y_{C_2H_2} \tag{12}$$

where S is the total soot surface area per unit volume,

$$S = \pi d_p^2 N \tag{13}$$

and the diameter of soot particle is calculated,

$$d_p = \left(\frac{6\rho Y_s}{\pi \rho_s N}\right)^{1/3} \tag{14}$$

Coagulation between soot particles is considered, and the rate of coagulation is given by

$$r_5 = \frac{1}{2}\beta N^2 \tag{15}$$

The coagulation constant, β, is determined from harmonic mean of free-molecular collision frequency β_{fm} and near continuum collision frequency β_{nc},

$$\beta = \frac{\beta_{fm}\beta_{nc}}{\beta_{fm} + \beta_{nc}} \tag{16}$$

$$\beta_{fm} = 4a\sqrt{\frac{6k_B T d_p}{\rho_s}} \tag{17}$$

$$\beta_{nc} = \frac{8k_B T}{3\mu}(1 + 1.257Kn) \tag{18}$$

where k_B is the Boltzmann constant (1.38×10^{-23} J/K) and Kn is the Knudsen number.

The precursors are oxidized by,

$$PR + O_2 + 24H_2 \Rightarrow 2CO + 24C_2H_2 \tag{19}$$

$$r_6^{kin} = A_6 \exp(-T_6/T)\, Y_{PR} \frac{\rho Y_{O_2}}{W_{O_2}} \tag{20}$$

The oxidation of acetylene proceeds with

$$C_2H_2 + O_2 \Rightarrow 2CO + H_2 \tag{21}$$

$$r_7^{kin} = A_7 \exp(-T_7/T)\, Y_{C_2H_2} \frac{\rho Y_{O_2}}{W_{O_2}} \tag{22}$$

The soot particles are oxidized,

$$Soot + O_2 \Rightarrow smaller\ soot + 2CO \tag{23}$$

$$r_8^{kin} = 12\left[\frac{k_A p_{O_2}}{1 + k_A p_{O_2}} x_A + k_B p_{O_2}(1 - x_A)\right] S/\rho \tag{24}$$

where

$$x_A = [1 + (k_T/p_{O_2})]^{-1} \tag{25}$$

$$k_A = 20 \exp(-30/RT) \tag{26}$$

$$k_B = (4.46 \times 10^{-3}) \exp(-15.2/RT) \tag{27}$$

$$k_T = (1.51 \times 10^5) \exp(-97/RT) \tag{28}$$

$$k_z = 21.3 \exp(4.1/RT) \tag{29}$$

The mixing effects are considered with Magnussen's eddy-dissipation model (Magnussen and Hjertager, 1976) in calculating oxidation of precursor, acetylene and soot.

$$r_i^{mix} = c_1 \frac{\varepsilon}{k} Y_k \tag{30}$$

where c_i is taken to be 10.

The reaction rates of oxidation are determined by harmonic means of the kinetic reaction and

mixing.

$$r_i=\frac{r_i^{kin}r_i^{mix}}{r_i^{kin}+r_i^{mix}},\ i=6,\ 7 \text{ and } 8 \tag{31}$$

The rates of change of mass fraction of species are calculated simultaneously,

$$\frac{dY_F}{dt}=-r_1-r_2 \tag{32}$$

$$\frac{dY_{O_2}}{dt}=-\frac{W_{O_2}}{W_{PR}}r_6-\frac{W_{O_2}}{W_{C_2H_2}}r_7-\frac{W_{O_2}}{W_C}r_8 \tag{33}$$

$$\frac{dY_{H_2}}{dt}=15\frac{W_{H_2}}{W_F}r_1+8\frac{W_{H_2}}{W_F}r_2+\frac{W_{H_2}}{W_{C_2H_2}}r_4+\frac{W_{H_2}}{W_{C_2H_2}}r_7-24\frac{W_{H_2}}{W_{PR}}r_6 \tag{34}$$

$$\frac{dY_{CO}}{dt}=2\frac{W_{CO}}{W_{PR}}r_6+2\frac{W_{CO}}{W_{C_2H_2}}r_7+2\frac{W_{CO}}{W_C}r_8 \tag{35}$$

$$\frac{dY_{C_2H_2}}{dt}=7\frac{W_{C_2H_2}}{W_F}r_2-r_4-r_7+24\frac{W_{C_2H_2}}{W_{PR}}r_6 \tag{36}$$

$$\frac{dY_{PR}}{dt}=0.28\frac{W_{PR}}{W_F}r_1+\left.\frac{dY_{PR}}{dt}\right|_{INC}-r_6 \tag{37}$$

$$\frac{dY_{soot}}{dt}=\left.\frac{dY_{soot}}{dt}\right|_{INC}+2\frac{W_C}{W_{C_2H_2}}r_4-r_8 \tag{38}$$

$$\frac{dN}{dt}=\rho\frac{N_A}{W_{PR}}\cdot\left.\frac{dY_{soot}}{dt}\right|_{INC}-r_5 \tag{39}$$

To solve this system of ODEs, Eqs. (32)~(39), VODE ODE solver (Brown et al., 1989) was used. The VODE solves the initial value problem for stiff or nonstiff systems of first order ODEs with fixed-leading-coefficient implementation. Changes of the number density of soot and mass fractions of each species due to reactions are calculated by VODE solver. The soot model was incorporated with the KIVA-3V code (Amsden, 1999) and applied to the diesel engine. The specification of the engine and operating conditions are listed in Tables 2 and 3. The transportation of the number density of soot and mass fractions of each species with convection and diffusion are calculated by KIVA-3V main solver.

Table 2 Engine specification (Brown et al., 1989)

Engine type	Direct injection, Turbo charged 4 valves
Bore×stroke	140×152 (mm)
Displacement	2.34 (L)
Compression ratio	13
Type of injector	Unit injector 0.20 (mm)×8 (holes)
Spray angle	152 degrees

Table 3 Computational conditions (Brown et al., 1989)

Engine revolution (rpm)	1200
Swirl number	1.4
Amount of fuel (g/stroke)	0.053
Start of Injection (CA BTDC)	19, 11*, 3
Initial temperature (K)	430
Initial pressure (MPa)	0.23

* : baseline case

$$\frac{\partial\rho(N/N_A)}{\partial t}+\frac{\partial}{\partial x_j}\left(\rho u_j\frac{N}{N_A}\right)=\frac{\partial}{\partial x_j}\left(D\frac{\partial(N/N_A)}{\partial x_j}\right)+\left(\frac{d\rho(N/N_A)}{dt}\right) \tag{40}$$

$$\frac{\partial\rho Y_s}{\partial t}+\frac{\partial}{\partial x_j}(\rho u_j Y_s)=\frac{\partial}{\partial x_j}\left(D\frac{\partial Y_s}{\partial x_j}\right)+\left(\frac{d\rho Y}{dt}\right) \tag{41}$$

where N_A is the Avogadro number (6.023×10^{23} molecules/mol), and N is the soot number density (particles/cm^3).

Figure 2 shows the combustion chamber at TDC with computational meshes used in this study. It represents one-eighth of the engine combustion chamber since the injector has eight symmetric holes for spray. It has 29 cells in radial direction, 20 cells in azimuthal direction and 28 cells in axial direction. The computation is continued until the timing of exhaust valve opening (EVO), and it takes about 4 hours to calculate one case with a Pentium 4 PC.

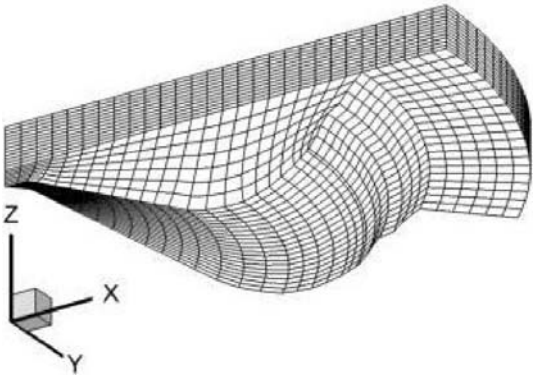

Fig. 2 Computational meshes for a combustion chamber at TDC

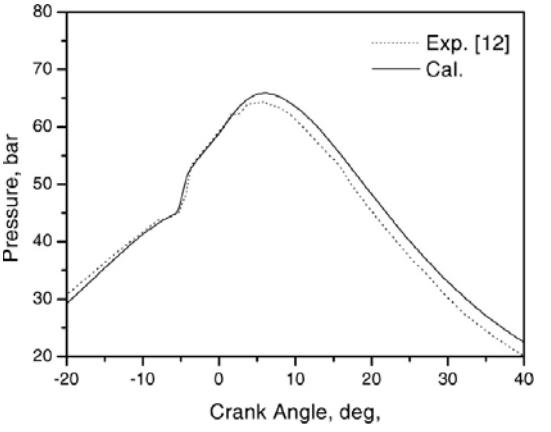

Fig. 3 Variation of cylinder pressure

3. Results and Discussions

Figure 3 shows variation of cylinder pressure during combustion. The calculated results of cylinder pressure from the model show good agreement with the experimental data, In the later part of combustion, the calculated cylinder pressure is higher than experimental data mainly due to underestimation of heat transfer from the cylinder. Fig. 4 shows normalized value of soot mass with experimental data using two-color optical pyrometry (Ishii et al., 2001). The results from calculation show slow formation of soot in the early part of combustion and active formation in the later part of combustion under higher cylinder temperature compared with the experimental measurements. Fig. 5 shows variation of soot mass in a cylinder during combustion. The soot is actively formed and grown during the combustion and reaches a peak near 8° ATDC. Then, it is decreased mainly due to oxidation and 60% of the peak is reduced at 20° ATDC.

Figure 6 shows distributions of equivalence ratio, temperature, formation rate of precursors and inception rate of soot. The injected fuel penetrates entire cylinder at TDC, and fuel rich core is developed inside the spray in Fig. 6(a). The flame is located near the stoichiometric equivalence ratio in Fig. 6(b). The precursors are actively formed inside the flame where mixture is rich in Fig. 6(c). The soot is produced mainly inside the flame where precursors are concentrated in Fig. 6(d).

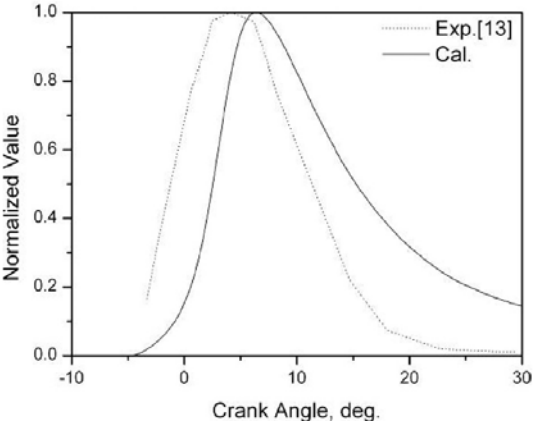

Fig. 4 Variation of normalized soot mass

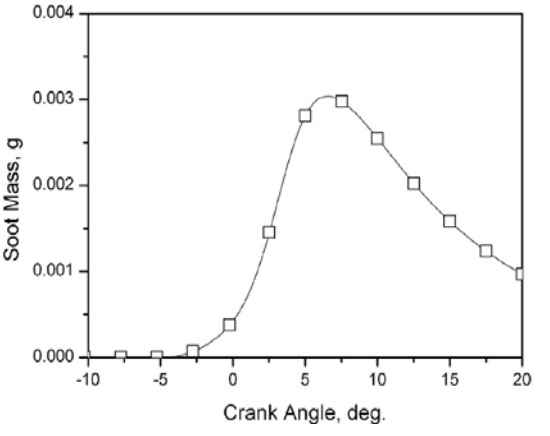

Fig. 5 Variation of soot mass in a cylinder

The precursors in the fuel-rich core are transformed into soot particles quickly because of hig-

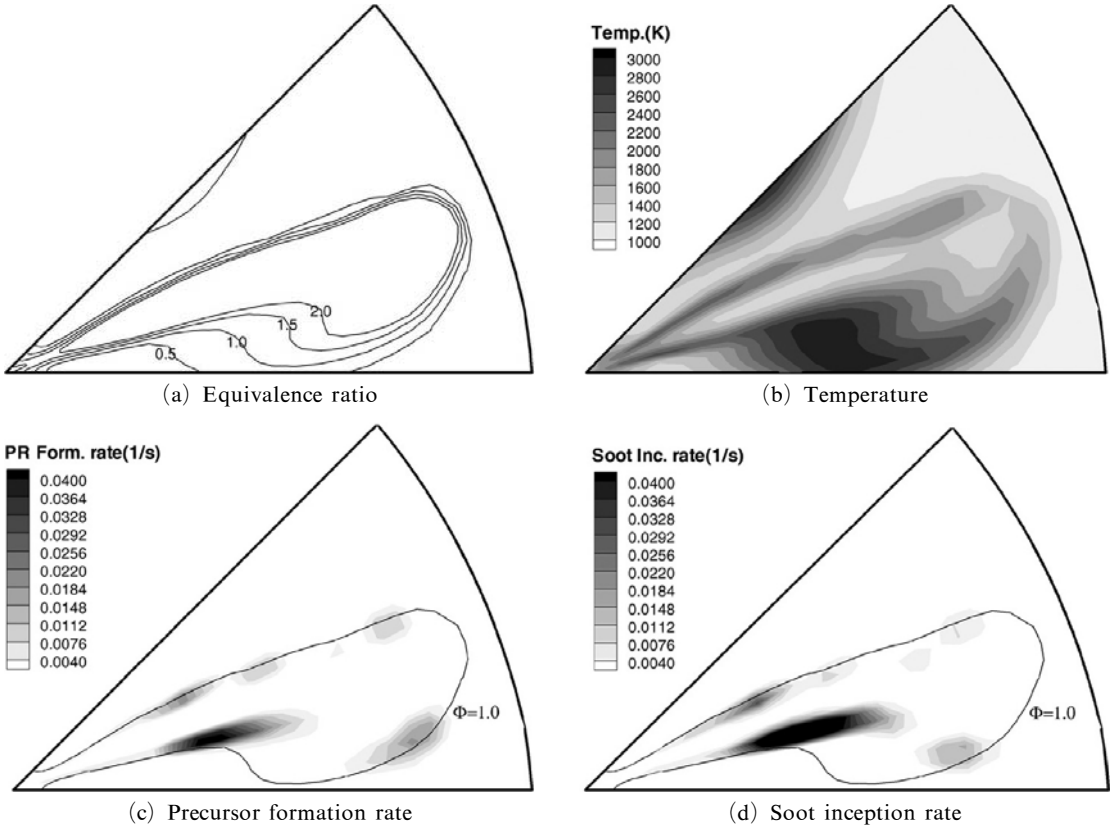

(a) Equivalence ratio (b) Temperature

(c) Precursor formation rate (d) Soot inception rate

Fig. 6 Results at TDC

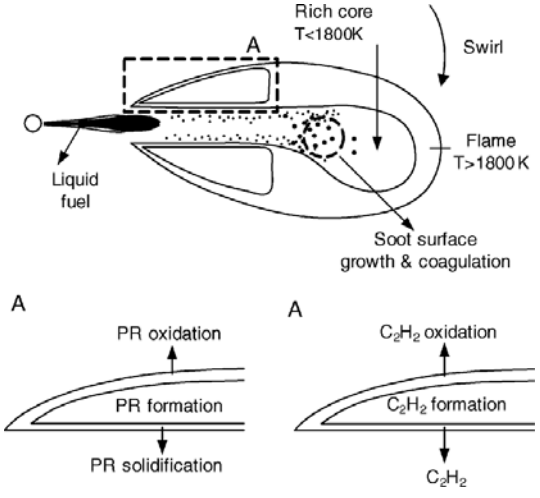

Fig. 7 Schematic diagram of soot formation in the spray (Ishii et al., 2001)

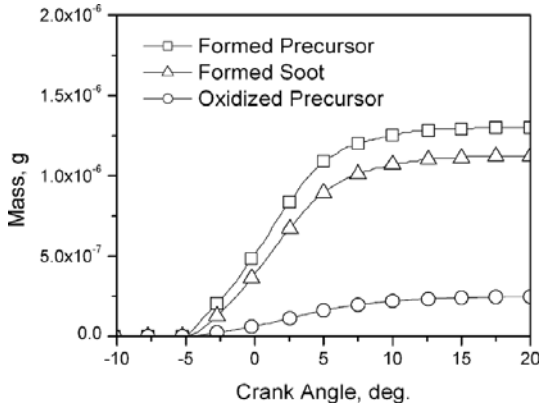

Fig. 8 Variation of precursors and soot

her concentration. The inception of soot in the spray is described by Lee (2004). In Fig. 7, the liquid fuel droplets are rapidly evaporated after breakup in the spray and mixed with the surrounding air by the swirling flow. The flame is located along the region of stoichiometric mixture ratios. The precursors in the core of flame are changed into soot particles because of high concentration. The incepted soot particles are then coagulated

and grown by acetylene. Fig. 8 shows variation of precursors and soot mass inside a cylinder. The precursors are actively produced in the early part of combustion and quickly converted to soot particles. At 5° ATDC, the production of precursors is ceased, and the generation of soot is terminated. Fig. 9 shows the change of number density of soot. The number density of soot is peaked near TDC and starts to decrease rapidly because of oxidation. After 10° ATDC, the number density of soot shows slow decrease due to the coagulation.

Figure 10 shows variation of cylinder temperature for different injection timings. When the start of injection (SOI) timing is advanced to 19° BTDC, the ignition delay is increased due to the low air temperature, and the fuel mixed with air during the ignition delay is burned abruptly after autoignition. With the effects of compression, this results in the peak cylinder temperature of 1650 K at 5° ATDC. When SOI timing is retarded to 3° BTDC, the ignition delay is shortened and peak of cylinder temperature is much decreased because of expansion. Fig. 11 shows distributions of equivalence ratio, temperature and formation rate of precursors and inception rate of soot for different injection timings at the crank angle when the inception rate of soot is maximum in each case. When injection timing is advanced to 19° BTDC, the ignition delay is increased and mixing between fuel and air are enhanced resulting in the uniform distribution of equivalence ratios as shown in Fig. 11(a). In this case, the formation of precursor is reduced because of large stoichiometric area and the inception of soot is suppressed due to high temperature as shown in Fig. 11 (b). On the other hand, for the injection timing at 11° BTDC or 3° BTDC, more fuel is concentrated in the core of spray which results in the high formation rates of precursors. Much of these precursors are transformed to soot under low saturation pressure. The effect of injection timing on soot number density is shown in Fig. 12. When the injection timing is advanced to 19° BTDC, the soot number density is decreased by 25% mainly due to reduced precursors and slow solidification. When the injection timing is retarded to 3° BTDC, the soot number density is reduced by 25% because of reduced precursors under low cylinder temperature. Fig. 13 shows productions of precursors and soot for the different injection timings. When the injection timing is advanced, the production of precursors and incepted soots are similar to the case of standard timing. When the injection timing is retarded to 3° BTDC, the formation of precursors is reduced because of low cylinder temperature but the production of soot from the precursor is relatively active because of low saturation pressure. The formed acetylene and the mass of soot are shown in Fig. 14. The acetylene and mass of soot are decreased for the advanced injection timing at 19° BTDC because of large stoichiometric area. For the retarded injection timing at 3° BTDC, the production of acetylene is delayed until the cylinder temperature

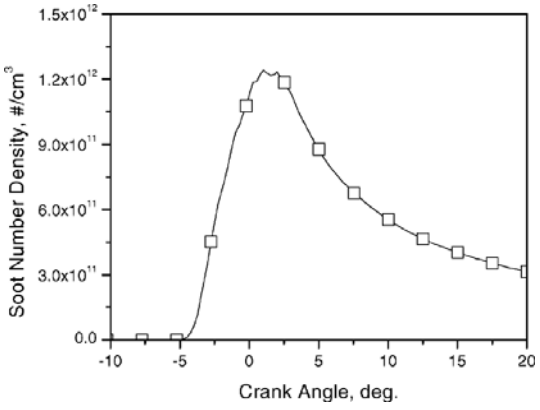

Fig. 9 Variation of soot number density in cylinder

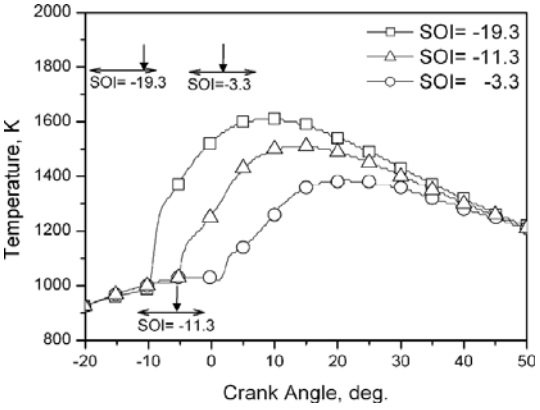

Fig. 10 Effect of injection timings on cylinder temperature

reaches 1200 K. The total production of acetylene and soot by acetylene for the retarded injection timing at 3° BTDC is comparative with that for standard injection timing. In each injection case, a half of the total acetylene is consumed for the growth of soot. Fig. 15 shows variations of soot with oxidized soot for the different injection timings. When injection timing is advanced to 19° BTDC, the formed soot is immediately oxidized due to the high cylinder temperature. When the injection timing is retarded to 3° BTDC, oxidation of soot is relatively slow because of low cylinder temperature which results in the increased soot emissions.

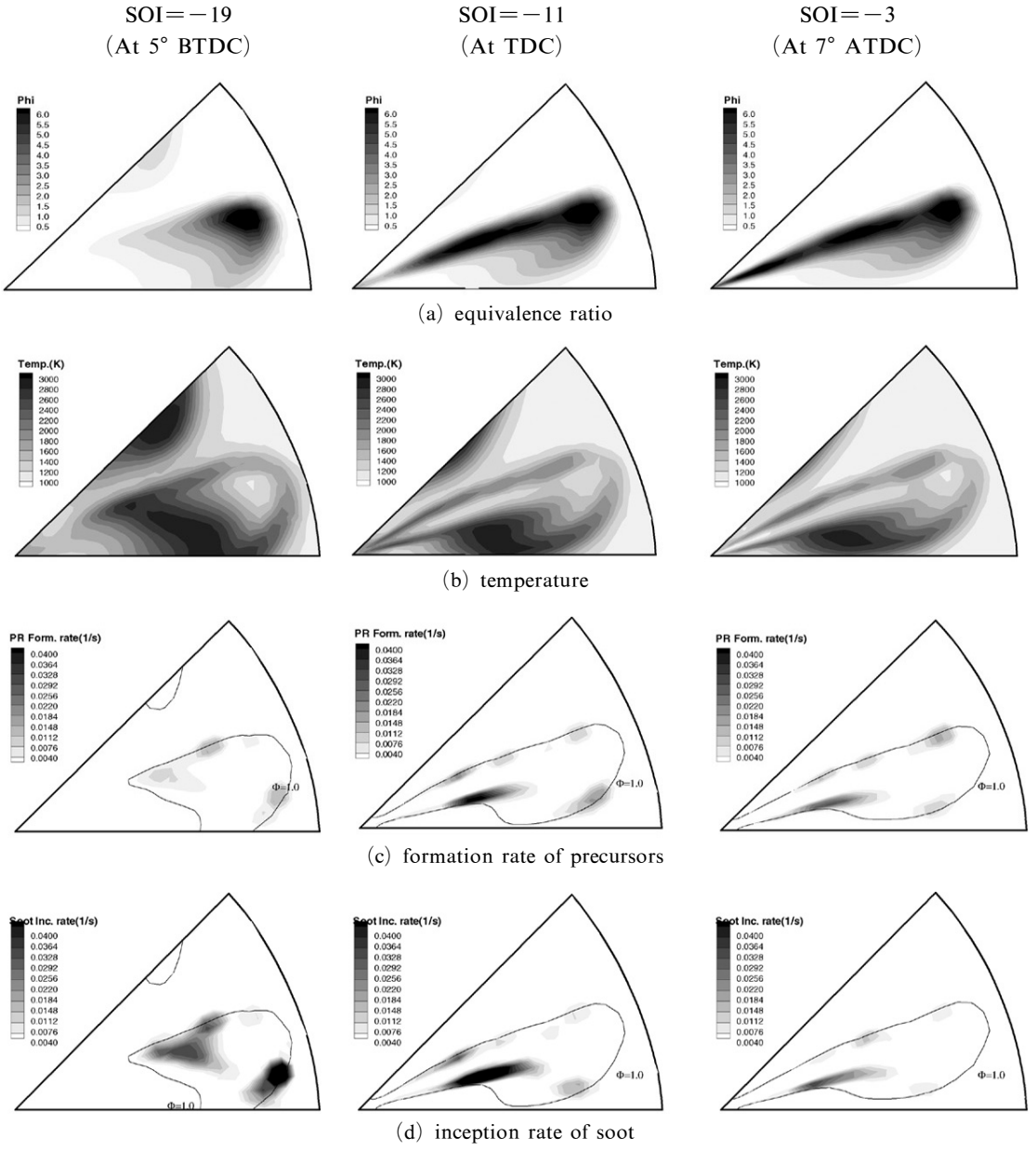

Fig. 11 Comparisons of distributions of temperature, equivalence ratio, formation rate of precursors and inception rate of soot for different SOI's

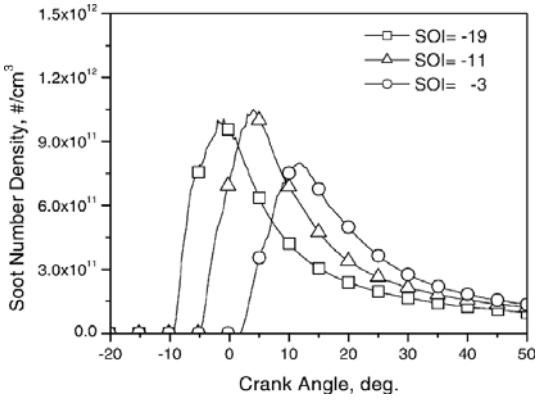

Fig. 12 Effect of injection timing on soot number density

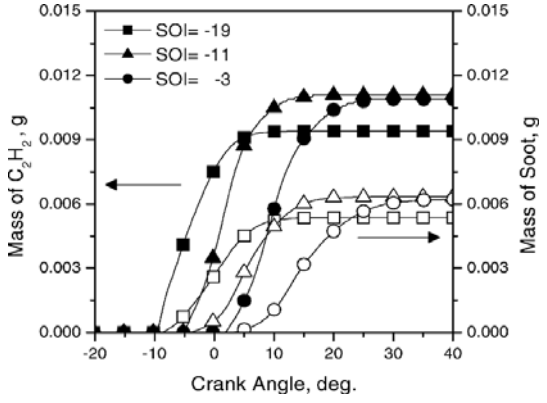

Fig. 14 Variation of acetylene and soot mass for different injection timings

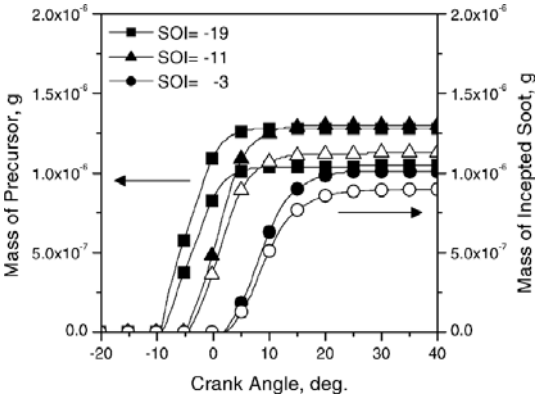

Fig. 13 Variations of precursors and incepted soot for the different injection timings

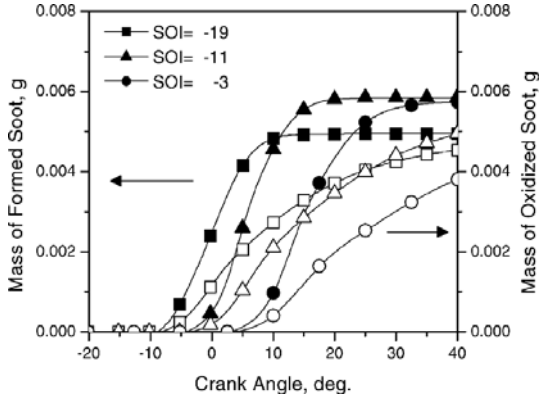

Fig. 15 Variation of oxidized soot for different injection timings

4. Conclusions

The soot inception from the precursors is calculated using the phase change of carbon atoms under the saturation condition. With the phase equilibrium model and distributions of fuel and local temperatures inside a cylinder, the formation and oxidation of soot can be explained reasonably.

The effect of injection timing on the soot formation is studied by this model. When the injection timing is advanced, the formations of precursors and acetylene are decreased because of the large stoichiometric area. The inception of soot from precursors is also reduced due to high saturation pressure inside the flame. When the injection timing is retarded, the soot emissions are increased mainly due to slow oxidation.

Acknowledgments

The authors would like to thank Korea Science & Engineering Foundation for their support and help with this work.

References

Amsden, A. A., 1999, *KIVA-3V Release2 : Improvements to KIVA-3V*, Los Alamos National Laboratory report, LA-UR-99-915.

Brown, P. N., Byrne, G. D. and Hindmarsh, A. C., 1989, "VODE : A Variable Coefficient ODE Solver," *SIAM J. Sci. Stat. Comput.*, 10, pp. 1038~

1051. Also, LLNL Report UCRL-98412.

Frenklach, M., 2002, "Reaction Mechanism of Soot Formation in Flames," *Phys. Chem. Chem. Phys*., Vol. 4, pp. 2028～2037.

Hampson, G. J., 1997, "A Theoretical and Experimental Study of Emissions Modeling for Diesel Engines with Comparisons to In-Cylinder Imaging," *Ph. D. Thesis*, University of Wisconsin-Madison.

Heywood, J. B., 1988, "Internal Combustion Engine Fundamentals," p. 492, pp. 567～571, pp. 635～647, McGraw Hill book company, International Edition.

Hiroyasu, H. and Nishida, N., 1989, "Simplified Three-Dimensional Modeling of Mixture Formation and Combustion in a D.I. Diesel Engine," SAE paper No. 890269.

Ishii, H., Goto, Y., Kazakov, A. and Foster, D. E., 2001, "Comparison of Numerical Results and Experimental Data on Emission Production Processes in a Diesel Engine," SAE paper No. 2001-01-0656.

Kazakov, A. and Foster, D. E., 1998, "Modeling of Soot Formation During DI Diesel Combustion Using a Multi-Step Phenomenological Model," SAE paper No. 982463.

Lee, S. S., 2004, "Analytical Study on Soot Emissions in a Diesel Engine," *Ph.D. Thesis*, Sungkyunkwan University.

Leung, K. M. and Lindstedt, R. P., 1991, "A Simplified Reaction Mechanism for Soot Formation in Nonpremixed Flames," *Combustion and Flame*, Vol. 87, pp. 289-305.

Liu, F., Guo, H., Smallwood, G. J. and Gulder, O. L., 2002, "A Numerical Study of the Influence of Transport Properties of Inert Diluents on Soot Formation in a Coflow Laminar Ethylene/Air Diffusion Flame," *Proceedings- Combustion Institute*, Vol. 29, No. 1, pp. 2359～2366.

Magnussen, B. F. and Hjertager, B. H., 1976, "On Mathematical Modeling of Turbulent Combustion with Special Emphasis on Soot Formation and Combustion," *16th Symposium (International) on Combustion, Combustion Institute*, pp. 719～729.

Pierson, H. O., 1993, *Handbook of Carbon*, Graphite, Diamond and Fullerenes, Noyes Publication.

Surovikin, V. F., 1976, "Analytical Description of the Processes of Nucleus Formation and Growth of Particles of Carbon Black in the Thermal Decomposition of Aromatic Hydrocarbons in the Gas Phase," *Khimiya Tverdogo Topliva*, Vol. 10, pp. 112～122.

Tao, F., Golovitchev, V. I. and Chomiak, J., 2004, "A Phenomenological Model for the Prediction of soot Formation in Diesel Spray Combustion," *Combustion and Flame*, 136.